Fluorinated polymer membranes as advanced substrates for portable analytical systems and their proof of concept for colorimetric bioassays

Ricardo Brito-Pereira[a,b], *André S. Macedo*[b,c], *Carmen R. Tubio*[d], *Senentxu Lanceros-Méndez*[b,d,e*], *Vanessa F. Cardoso*[a,b*]

[a]CMEMS-UMinho, Universidade do Minho, Campus de Azurém, 4800-058 Guimarães, Portugal

[b]CF-UM-UP, Centro de Física das Universidades do Minho e Porto, Universidade do Minho, Campus de Gualtar, 4710-057 Braga, Portugal

[c]IB-S, Institute of Science and Innovation for Bio-Sustainability, Universidade do Minho, Campus de Gualtar, 4710-057 Braga, Portugal

[d]BCMaterials, Basque Center for Materials, Applications and Nanostructures, UPV/EHU Science Park, 48940 Leioa, Spain

[e]IKERBASQUE, Basque Foundation for Science, 48009 Bilbao, Spain

* senentxu.lanceros@bcmaterials.net; * vanessa@dei.uminho.pt

KEYWORDS: microfluidic paper-based analytical devices, poly(vinylidene-co-trifluorethylene), polymer, microfluidic, portable analytical systems.

ABSTRACT: Portable analytical systems are increasingly required for clinical analysis or environmental monitoring, among others, being materials with tailored physicochemical properties among the main needs for successful functional implementation. This manuscript describes the processing of fluorinated poly(vinylidene-*co*-trifluorethylene), P(VDF-TrFE), membranes with tailored morphological and physicochemical properties to be used as microfluidic substrates for portable analytical systems, commonly called point-of-care, POC, systems in the medical field. The morphology of the developed membranes includes spherulitic, porous, randomly oriented and oriented fibres. Further, the processed hydrophobic P(VDF TrFE) membranes were post-treated by oxygen plasma to become superhydrophilic. The influence of morphology and plasma treatment on the physicochemical properties and capillary flow rates were evaluated. Microfluidic systems were then designed and printed by wax-printing for the colorimetric quantification of glucose. The systems comprise eight reaction chambers, each glucose concentration (25, 50, 75, and 100 $mg.dL^{-1}$) being measured in two reaction chambers separately and at the same time. The results demonstrate the suitability of the developed microfluidic substrates based on their tailorable morphology, improved capillary flow rate, wax print quality, homogeneous generation of colorimetric reaction and excellent mechanical properties. Finally, the possibility of being re-used, along with their electroactive properties, can lead to a new generation of microfluidic substrates based on fluorinated membranes.

1. Introduction

Portable devices for expedite and easy medical diagnosis are increasingly demanded as a suitable tool to detect various diseases. Those devices allow early diagnosis *in situ* and can be accessible to a large number of people without the need for complex laboratory equipment. Further, they are particularly valuable for preliminary analysis before further evaluation or to evaluate on-going processes, allowing to improve healthcare assistance [1]. Further, they have been also used in other research fields such as environmental safety [2], animal health [3] or food quality [4], among others.

In particular, in times of pandemic outbreaks, as the one we are experiencing nowadays, access to low-cost, easy to handle diagnostic methods that can be distributed quickly among the population is becoming essential to promote mass diagnosis and provide high quality control concerning the spread of the disease at an early stage [5] .

It is particularly relevant that these tools address the ASSURED (Affordable, Sensitive, Specific, User-friendly, Rapid and robust, Equipment-free and Deliverable to end-users) guidelines for the development of point-of-care (POC) devices as defined by the World Health Organization (WHO). Devices with low manufacturing cost, low sample volume and with minimal user manipulation are then best suited to satisfy these guidelines [6 7].

Microfluidic paper-based analytical devices (µPADs), introduced by the Whitesides group in 2007 [8], are a relevant option for the development of such tools. Microfluidic platforms have been fabricated from a wide array of materials such as silicon, glass or polymers that can be tailored into three-dimensional (3D) solid structures, as it is the case of polydimethylsiloxane (PDMS) and poly(methyl methacrylate) (PMMA), which possess overall high mechanical strength [9]. Cellulose paper features economical, compact and lightweight properties for the fabrication of µPADs.

Moreover, because of its superhydrophilic properties, passive capillary flow discards the need for an external pump [10]. Hydrophobic barriers can be printed to improve liquid flow through the substrate, allowing designs to guide solutions to different locations of the microfluidic platform for specific purposes. Several technologies may be used to implement these barriers, including wax and inkjet printing [9], photolithography [8], printed circuit technology [11] and screen-printing [12].

Nonetheless, commercial microfluidic substrates show disadvantages that include weak mechanical properties and the type of cellulosic paper has to be carefully selected: Commercial inkjet printing paper is unsuitable due to its low porosity and surface tension; filter paper such as *Whatman*^{TM} cellulose paper (the gold standard on point-of-care applications after its introduction [8]) may possess pores that are too large, preventing proper capillary flow [6]. More recently, *Hi-Flow Plus* nitrocellulose substrates from *Millipore* have emerged as an interesting alternative for microfluidic applications, allowing controlled capillary flow rate and thus sensitivity, depending on the specific type of membrane. However, it is expensive, must be handled very carefully to maintain the integrity the membrane and typically needs an external baking material to support the nitrocellulose structure. Thus, alternative microfluidic substrates are being explored, such as poly(L-lactic acid) (PLLA), an aliphatic semi-crystalline polyester known for its biocompatibility and biodegradability, in the form of electrospun membranes [13].

In this context, synthetic polymers, such as poly(vinylidene-*co*-trifluorethylene) (P(VDF-TrFE), a copolymer of poly(vinylidene fluoride) (PVDF), can be an interesting alternative to the commonly used microfluidic substrates. P(VDF-TrFE) presents excellent mechanical properties regardless of the processing method and resulting morphology, is characterized by high chemical and thermal resistance, as well as biocompatibility [14]. Furthermore, it has the highest dielectric constant among polymers and it is also an electroactive, including piezo-, pyro- and ferroelectricity, that

crystallizes directly into the β phase, independently of the processing conditions, when the TrFE content is 20% mol or higher. Its piezoelectric coefficient d_{33} is −38 pC.N^{-1} [15]. Thus, P(VDF-TrFE) has been used in microfluidic applications for the development of piezoelectric micropumps [16], flow [17] and temperature [18] sensors or acoustic actuators [19].

P(VDF-TrFE)-based membranes can be manufactured with several microstructures using a variety of processing methods as described in a previous review [14]. One way to process this polymer is in the form of porous films. Techniques based on phase inversion allow porosity and pore size control, as well as industrial scalability. Two specific methods based on this principle were used in the present work: a)) non-solvent induced phase separation (NIPS), where the liquid or vapour phase in the polymer solution is diffused by submerging it in a nonsolvent coagulation bath, giving rise to polymer-rich and poor zones which lead to pore formation, and b)) thermally induced phase separation (TIPS), where the appearance of these structures is due to a polymer-solvent phase separation at a specific temperature, that occurs before solvent evaporation and polymer crystallization [20].

Electrospinning (ES) is another versatile and highly reproducible technique to produce polymer fibre membranes by applying a high electrical field to a droplet of polymer solution or melt. By controlling the characteristics of the polymer solution and processing conditions, a stable procedure can be achieved to obtain fibre mats with tailorable fibre diameter and orientation [21]. In the present work non-oriented and oriented electrospun P(VDF-TrFE) membranes were thus also processed by ES .

P(VDF-TrFE) is a hydrophobic polymer, which prevents capillary flow through membranes or films. One way to overcome this limitation involves surface plasma treatments, which introduce

morphological modifications and/or functional groups into the surface of the material by exposing it to plasma of a selected composition (Ar, O_2 and N_2 are some of the most used). Thus, hydrophobic membranes can be converted into superhydrophilic ones [22], due to the cleavage of C-F and C-H bonds which are replaced by C=O, -OH and -COOH hydrophilic groups [23].

In order to provide novel and complementary microfluidic substrates to the limited commercially ones, this work evaluates the potential of P(VDF-TrFE) membranes processed in a variety of morphologies for manufacturing portable analytical devices. Thus, in the present work the suitability, advantages and limitations of P(VDF-TrFE) to be used as microfluidic substrates in the form of oriented and randomly-oriented electrospun membranes, as well as in the form of porous membranes obtained by NIPS and TIPS techniques, has been addressed. The processed membranes were compared to the commonly used *Whatman^{TM} no. 1* cellulose filter paper and *Hi-Flow Plus membranes HF090* from *Millipore*. Microfluidic platforms based on the P(VDF-TrFE) substrates were also designed and tested for the quantification of glucose. To our knowledge, this is the first time that superhydrophilic P(VDF-TrFE) substrates have been used for microfluidic applications.

2. Experimental section

2.1. Materials

P(VDF-TrFE) 70/30 powder (70 mol% vinylidene fluoride monomer and 30 mol% trifluoroethylene) was obtained from *Piezotech* (Pierre-Bénite, France). N,N-dimethylformamide (DMF) and absolute ethanol were obtained from *Merck*. *Whatman^{TM}* qualitative filter paper

grade 1 and *Hi-Flow Plus HF090* were acquired from *GE Healthcare* and *Millipore*, respectively. Distilled water was prepared in our laboratory. All reagents and solvents were used as received.

2.2. Sample preparation

Several processing techniques and post-treatment protocols were employed to produce P(VDF-TrFE) membranes with tailored morphological and physicochemical properties suitable for microfluidic device development [14]. NIPS technique was used to produce P(VDF-TrFE) membranes using ethanol as a weak non-solvent in order to tune the liquid-liquid demixing process to produce samples with large spherical microstructures, similar to commercial *Hi-Flow Plus* substrates from *Millipore* [24]. On the other hand, TIPS technique was used to produce pore-based microstructures as an alternative morphology [24]. Further, ES has been used to obtain randomly oriented P(VDF-TrFE) fibre membranes, mimicking the morphology of commercial *Whatman™ no.1* [25], and oriented electrospun membranes, in order to study the effect of fibre orientation [15].

As the hydrophobic nature of P(VDF-TrFE) membranes hinders their use as microfluidic substrates, the as-processed membranes were submitted to a post-treatment with oxygen plasma and its effect on the physicochemical properties of the membranes was evaluated.

2.2.1. P(VDF-TrFE) solution preparation

A 20 wt% solution of P(VDF-TrFE) powder dissolved in DMF was prepared under magnetic stirring. A slight heating at 40 ºC was applied in the first 30 min of dissolution to speed up the process and the solution was then allowed to cool under magnetic stirring until a homogeneous (without air bubbles) and transparent solution was obtained, which took no longer than 3 h. The polymer concentration was defined in order to obtain a solution compatible with the processing techniques and conditions in order to obtain the membranes [14].

2.2.2. Non-solvent induced phase separation

The P(VDF-TrFE) solution was spread on clean and polished glass substrates (15 x 10 cm) by means of a hand-casting knife with a 450 µm gap. Then, the coated substrates were immersed in a coagulation bath composed by absolute ethanol for approximately 5 min at a temperature of 25 ºC controlled by a hot-plate (*Präzitherm PZ23-2*) and a digital thermometer (*Elitech WT-1*), until complete crystallization, after which the films peeled off the glass substrates. Then, it remains immersed for another 5 min in the coagulation bath before being transferred to a pure distilled water bath (also at 25 ºC) to guarantee total removal of residual solvent (. Finally, the membranes were left to dry at room temperature for 48 h [26]. The process is illustrated in Figure 1a. These membranes will be identified as NIPS membranes.

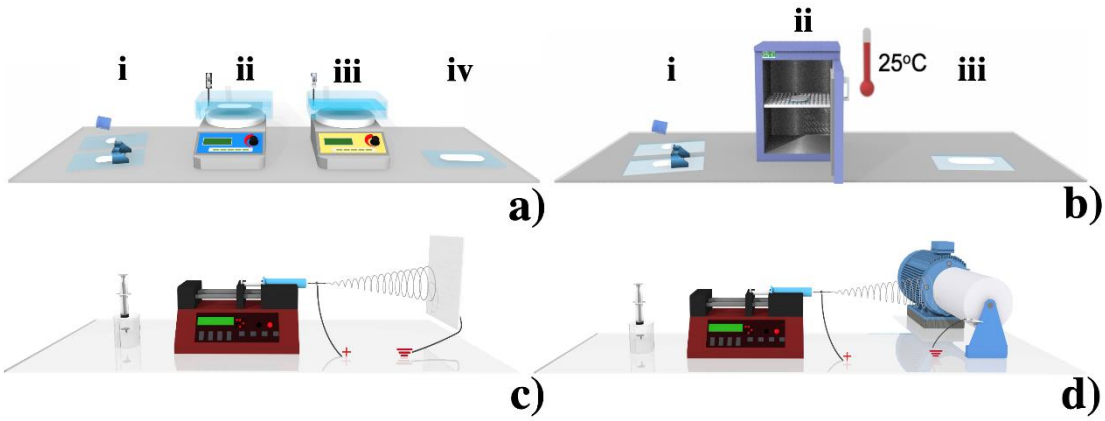

Figure 1. Schematic representation of the processing of a) P(VDF-TrFE) membranes by NIPS using ethanol as non-solvent: i. spreading of the polymer solution on a glass substrate by means of a hand-casting knife with a 450 µm gap; ii. immersion in a coagulation bath composed of ethanol at 25 ºC; iii. transfer to a bath of pure distilled water at 25 ºC; iv. drying at room temperature for 48 h. b) P(VDF-TrFE) membranes by TIPS: i. spreading of the polymer solution on a glass substrate by means of a hand-casting knife with a 450 µm gap; ii. placement within an oven at 25 ºC for 48 h; iii. dry sample. c) Randomly oriented electrospun P(VDF-TrFE) membranes by ES: filling the syringe with the polymeric solution and collecting the electrospun fibres on a grounded static plate collector under a high voltage. d) Oriented electrospun P(VDF-TrFE) membranes by ES: filling the syringe with the polymer solution and collecting the electrospun fibres on a grounded rotating drum collector under a high voltage.

2.2.3. Thermally induced phase separation

The P(VDF-TrFE) solution was spread on clean and polished glass substrates (15 x 10 cm) by means of a hand-casting knife with a 450 µm gap, similarly to the NIPS process. Then, the

coated substrates were placed into an oven (*JP SELECTA Digitronic-TFT*) to maintain a controlled temperature of 25 ºC for 48 h until fully dried. In the TIPS method, the PVDF-based physicochemical and morphological characteristics can be anticipated by the phase diagram of the polymer and solvent binary systems, in which the regions of miscibility and phase separation are identified [27]. Lower drying temperatures are associated with lower evaporation rates of the solvent, leading to highly porous membranes [14]. The process is illustrated in Figure 1b and these processed membranes will be identified as TIPS membranes.

2.2.4. Randomly oriented electrospun fibre mats

The P(VDF-TrFE) solution was transferred to 10 mL disposable syringes fitted with a blunt steel needle with an inner diameter of 500 μm and placed in a syringe pump (*New Era NE-1000*). Electrospinning was conducted using a high voltage power supply (*Glassman PS/FC30P04*) set at 15 kV and the solution was pumped at a flow rate of 0.5 $mL.h^{-1}$. The resulting randomly oriented electrospun P(VDF-TrFE) membranes were collected on a grounded 20 x 15 cm static plate collector placed 15 cm away from the needle. The process is illustrated in Figure 1c and the processed membranes will be identified as RO-ES membranes.

2.2.5. Oriented electrospun fibre mats

Oriented electropun P(VDF-TrFE) membranes were obtained after a process similar to the one described in section 2.2.4 except for the use of a grounded rotating drum collector, which was set

at a speed of 1500 rpm. The process is illustrated in Figure 1d and the processed membranes will be identified as O-ES membranes.

2.3. Surface modification by plasma treatment

The inherent hydrophobic characteristics of P(VDF-TrFE) constitute a limitation for its use as microfluidic substrates in portable analytical systems, as previously mentioned. Thus, P(VDF-TrFE) membranes were subjected to plasma treatment in order to obtain superhydrophilic membranes [28]. The success of plasma treatment is associated with an adequate selection of the plasma atmosphere (O_2, Ar, N_2 or others), treatment duration and applied power. Oxygen is one of the most reactive elements and can generate hydrophilic carboxyl groups on the polymer surface [29]. Thus, surface treatments were conducted in a plasma chamber (*Diener Electronics Zepto*) equipped with a 40 kHz radio frequency plasma generator. The base pressure before the application of the plasma was 20 Pa. A plasma power of 100 W was then applied for 10 min using oxygen under a total pressure of 80 Pa. This procedure was performed on both surfaces of the P(VDF-TrFE) membranes. These parameters were defined according to previous studies and further optimization to guarantee non-significant morphological changes and superhydrophilic properties stable over time [1330]. The processed P(VDF-TrFE) membranes with and without oxygen plasma treatment will be identified as w/ and w/o plasma, respectively.

2.4. Sample characterization

2.4.1. Physicochemical characterization

The morphology of the processed P(VDF-TrFE) membranes and commercial substrates were characterized by scanning electron microscope (SEM, *Hitachi S-4800*). Samples were previously sputtered (*Polaron SC502*) with a thin gold layer. Mean fibre diameter was calculated from measuring approximately 50 fibres using *ImageJ* software.

The porosity of the P(VDF-TrFE) membranes was measured by liquid displacement method using a pycnometer [31 32]. The weight of the pycnometer filled with ethanol was measured and labelled as W_1. The P(VDF-TrFE) membranes, whose weight was W_s, were immersed in ethanol; after the sample was saturated by ethanol, additional ethanol was added to fill the volume of the pycnometer. Then, the pycnometer was weighted and labelled as W_2. The sample filled with ethanol was then taken out of the pycnometer and the residual weight of the ethanol and the pycnometer was labelled W_3. The porosity of the membrane was calculated according to $\varepsilon = (W_2 - W_3 - W_S)/(W_1 - W_3)$. The porosity of each membrane was obtained as the average of the values determined in three samples. Absolute ethanol, as a non-solvent of PVDF, was used as displacement liquid since it can penetrate in the pores of the membranes and the electrospinning fibres, not inducing shrinking or swelling. The assays were performed on hydrophobic P(VDF-TrFE) membranes before plasma treatment, since plasma treated membranes absorb the ethanol on the polymer matrix, may lead to porosity measurement errors.

Differential scanning calorimetry (DSC) was performed with a *Perkin-Elmer 6000*. P(VDF-TrFE) samples weighing approximately 6 mg were placed into 40 µL aluminium pans and then heated from 30 to 200 ºC at a rate of 10 ºC.min^{-1}. The degree of crystallinity (X_C) was calculated after $X_C = (\Delta H_m/\Delta H_0) \times 100$, where ΔH_m corresponds to the melting enthalpy of the samples and ΔH_0 is the melting enthalpy for 100% crystalline P(VDF-TrFE) (91.45 J.g^{-1}) [33].

Mechanical properties were evaluated in the tensile mode with a *Shimadzu AD-IS* universal testing set up with a load cell of 50 N. 15 mm long and 10 mm wide samples were stretched at a rate of 1 $mm.min^{-1}$. O-ES membranes were stretched along the direction of the fibres. Average sample thickness values are: 120 µm for *Whatman™ no.1* and 110 µm, 103 µm, 92 µm and 81 µm for NIPS, TIPS, RO-ES and O-ES P(VDF-TrFE) membranes, respectively, measured using a *Fischer Dualscope MPOR*. The stress-strain measurements were performed in triplicate on dry and wet samples, using 40 µL of water in the latter. The assays were not performed on the *Millipore HF090* substrates as it is a laminated membrane with backing material that prevents the determination of the Young modulus of the nitrocellulose membrane.

Fourier-transformed infrared spectroscopy measurements in attenuated total reflectance mode (FTIR-ATR) were performed at room temperature in all samples using a *Jasco FT/IR-6100* set up, from 400 to 4000 cm^{-1} using 64 scans and a resolution of 4 cm^{-1}.

2.4.2. Contact angle and capillary flow rate assays

Surface wettability was evaluated using the sessile drop method (Data-Physics OCA20) by measuring the contact angle (CA) of 3 µL ultrapure water drops on the commercial and processed P(VDF-TrFE) samples. Six measurements were carried out in each sample at different locations and the average and standard deviation were calculated. The measurements were repeated every week during 2 months, storing the samples under environment conditions.

Capillary tests were performed on all samples, including commercial ones. 2.5 cm long and 1 cm wide sample strips were cut and submerged vertically in liquid coloured solution (green food

dye) in order to visualize and determine the capillary flow. A segment of 0.5 cm was first submersed, and the time taken for the dye to travel across the remaining 2 cm of the sample in the antigravitational direction was measured. These tests allow an evaluation of the effect of fibre orientation, film porosity and oxygen plasma treatment on capillary flow rate, and ultimately the evaluation of the ability of the different materials to generate passive flows.

2.5. Proof-of-concept: glucose determination

Glucose assays based on colorimetric detection were performed using a glucose kit (*Trinder – Endpoint, FAR Diagnostic*). During the reaction, glucose is oxidised by glucose oxidase to gluconic acid and hydrogen peroxide. The latter reacts with phenol and 4-aminophenazone in the presence of peroxidase, producing a coloured complex whose colour intensity is directly proportional to the glucose concentration in the samples. Calibration curves were determined for all samples using glucose concentrations of 25, 50, 75, and 100 $mg.dL^{-1}$. This range of concentrations includes ranges of reference values for both new-born babies (20 to 80 $mg.dL^{-1}$) and adults (70 to 110 $mg.dL^{-1}$). A microfluidic system was designed using *SolidWorks 2020* and hydrophobic wax was printed using a *Xerox ColorQube 8870* printer, as illustrated in Figure 2. Wax-Printing, when compared to other methods commonly used to print point-of-care devices, presents several advantages such as not requiring specialized facilities, the process is rapid, inexpensive (each wax cartridge can print a large number of devices) and environmental friendly (no use of organic solvents throughout the fabrication process)[34–36].

After printing, the samples were placed on a hot plate at 100 ºC for 10 min for the wax to penetrate the substrates all the way through to the opposing surface in order to fabricate the barriers able to contain the fluids.

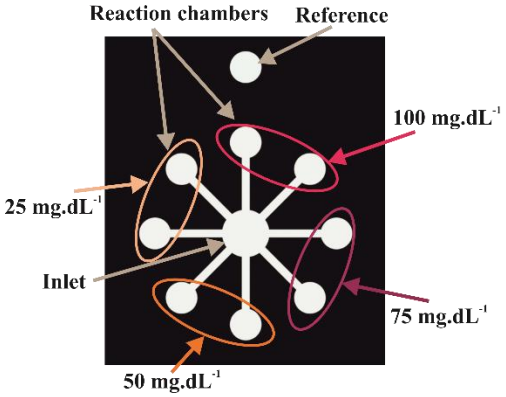

Figure 2. Design of the microfluidic system for the quantification of glucose. The glucose solution was placed in both reaction and reference chambers and the reagent in the inlet. The reagent flow by capillarity from the inlet to the reaction chamber to form a red/orange colour with intensity proportional to the concentration of glucose. The reaction chamber features a diameter of 8 mm and the channels a width of 1.2 mm.

Each microfluidic system comprises eight reaction chambers, with each glucose concentration being carried out in two reaction chambers separately and at the same time, as indicated in Figure 2. Three microfluidic systems were printed for each membrane in order to assess the reproducibility of the system. The reaction chambers were first functionalized using 15 µL of the glucose solution under study. After approximately 5 min, the reagent was introduced in the inlet of the microfluidic system, reaching the reaction chambers by capillarity. After 10 min of reaction, a red/orange colour with intensity proportional to the glucose concentration was

obtained. The substrates were then scanned (*Brother DCP-1610W*) and colour analysis was performed with the aid of *ImageJ* software by measuring mean grey values and the corresponding standard deviation on each reaction chamber of the microfluidic systems. These results were used to build the calibration curves [37].

3. Results and Discussion

P(VDF-TrFE) membranes with tailorable morphologies were processed by three distinct processing techniques. In the following sections, a complete physicochemical characterization of the processed P(VDF-TrFE) membranes will be presented, discussed and compared with commercial *Whatman™ no.1* and *Millipore HF090* membranes. The colorimetric quantification of glucose in the microfluidic systems printed on the membranes is also presented.

3.1. Physicochemical characterization

The use of membranes as microfluidic substrates is dependent on proper porous morphology [3839]. Representative SEM images of the processed and commercial membranes are presented in Figure 3.

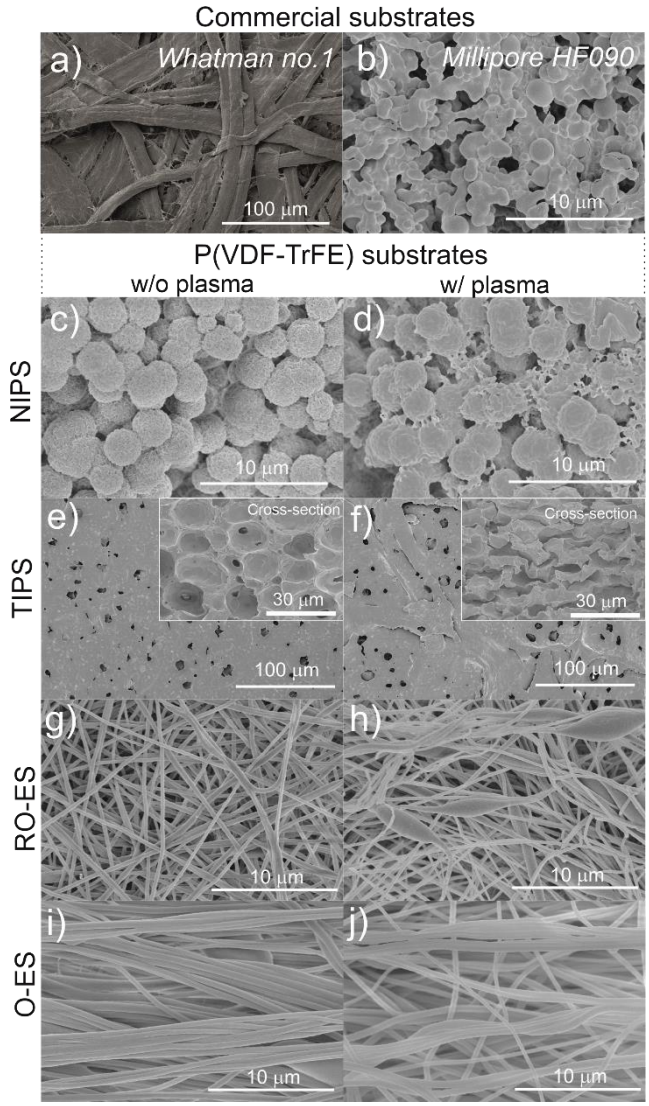

Figure 3. Representative SEM images of the processed P(VDF-TrFE) membranes before and after oxygen plasma treatment (above) together with commercial *Whatman™ no.1* and *Millipore HF090* substrates (below), for comparison.

Commercial *Whatman™ no.1* substrates (Figure 3a) are composed by randomly oriented cellulose microfibres with a flat structure (width in the order of tens of micrometer), which is associated with the manufacturing process of paper. On the other hand, *Millipore HF090* substrates (Figure 3b) feature a spherulitic-like nitrocellulose porous structure laminated with a

backing transparent material. Taking into account these microstructures, manufacturing techniques for P(VDF-TrFE)-based membranes were selected [14] in order to mimic the morphology of these commercial substrates and allowing to overcome some of their limitations, as will be discussed ahead. NIPS technique (Figure 3c) with ethanol as non-solvent was used to produce P(VDF-TrFE) membranes with morphology similar to *Millipore HF090*, however without the need for a support material. TIPS technique was also applied to obtain P(VDF-TrFE) membranes with an alternative porous microstructure characterized by well-defined round shaped pores (Figure 3e). Randomly oriented P(VDF-TrFE) fibre membranes were produced by ES (RO-ES) in order to mimic the morphology of the *Whatman^{TM} no.1* substrates (Figure 3g). Finally, oriented electrospun P(VDF-TrFE) fibres (O-ES) were also processed in order to evaluate the influence of fibre orientation in the physicochemical properties and passive capillary flow rate of the P(VDF-TrFE) membranes (Figure 3i). As the processed samples are hydrophobic, the P(VDF-TrFE) membranes were subjected to oxygen plasma treatment in order to tailor the polymer's surface wettability and to allow capillary flow. Oxygen plasma treatment allows to generate carboxyl group on the polymer surface by the incorporation of hydrophilic functional groups [30]. SEM images of the plasma treated P(VDF-TrFE) membranes (Figures 3d, 3f, 3h and 3j) reveal a slight change in the morphology of the membranes compared to the untreated P(VDF-TrFE) membranes, which is attributed to local polymer melting associated with the high power (100 W) and high exposure time (10 min) [13]. For instance, the plasma-treated P(VDF-TrFE) membranes obtained by NIPS (Figure 3d) present some melted and recrystallized regions in the interfaces between the spherulites, whereas the cross-section images of the plasma-treated P(VDF-TrFE) membranes obtained by TIPS (Figure 3f, inset) reveal a change in pore spherical shape, presenting more deformed and flattened pores. In turn, the overall 3D fibre

structure with smooth surfaces of the P(VDF-TrFE) membranes is maintained after plasma treatment, with average fibre diameter of 310 ±50 nm and 370±70 nm for the RO-ES (Figures 3g and 3h) and O-ES P(VDF-TrFE) (Figures 3i and 3j) membranes, respectively.

The porosity of the membranes is presented in Figure 4a.

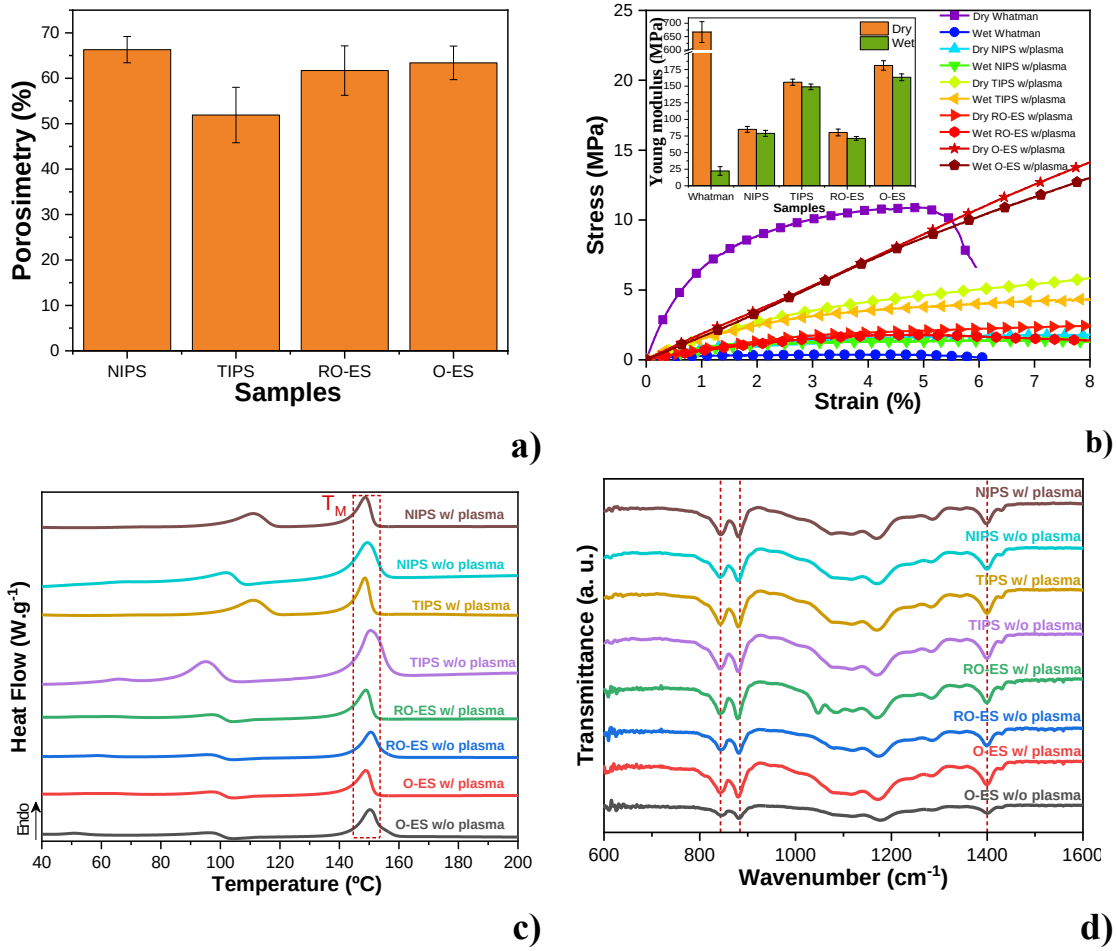

Figure 4. a) Porosity of the P(VDF-TrFE) membranes before oxygen plasma treatment; b) representative stress-strain curves up to 8% of strain and corresponding Young modulus with mean and standard deviation (inset) of the plasma treated P(VDF-TrFE) membranes; c) representative DSC curves and d) representative FTIR-ATR spectra of the P(VDF-TrFE) membranes before and after oxygen plasma treatment.

Independently of the processing method, all samples show degrees of porosity above 50%. No significant variations occur for the surface plasma treated samples (Figure 3).

In addition to the relevance of a porous morphology, membrane-based microfluidic substrates must keep adequate mechanical properties when wet during a functionalization process and/or after immersion in a solution containing the (bio)entity(ies) to be quantified. Stress-strain assays were conducted on dry and wet plasma treated P(VDF-TrFE) membranes and commercial *Whatman^{TM} no.1* microfluidic substrates. This experiment was not performed on *Millipore HF090* substrates as they possess backing material, which provides improved mechanical stability but prevents the determination of the mechanical properties of the nitrocellulose membrane itself.

The stress-strain mechanical curves are characterized by a linear elastic regime followed by a plastic regime after yielding where the material suffers permanent deformation after any increase in load or stress. By further stretching the samples, the rupture stress-strain is reached. Brittle materials, contrarily to ductile materials, typically feature little or no plastic deformation, fracturing within the linear elastic region. From the linear regime of the stress-strain curves, where materials are generally used, the Young's modulus has been obtained for each sample by applying Hooke's law. The characteristic stress-strain curves up to 8 % of strain along with the Young's modulus of the samples under study are presented in Figure 4b. Commercial *Whatman^{TM} no.1* substrates show almost no plastic regime in both dry and wet state, contrarily to the plasma-treated P(VDF-TrFE) membranes. Dry commercial *Whatman^{TM} no.1* substrates feature a more rigid behaviour with the highest Young's modulus of 667.2±38.8 MPa, strongly decreasing to 22.3±6.5 MPa when wet. In turn, the P(VDF-TrFE) membranes are mechanically stable before and after wetting, the wet samples nearly preserving the same elastic behaviour and

mechanical characteristics as the dry ones. In fact, wet treated P(VDF-TrFE) membranes only suffered a slight decrease of the Young's modulus compared to dry treated P(VDF-TrFE) membranes, being the wet treated RO-ES P(VDF-TrFE) and the dry treated O-ES P(VDF-TrFE) membranes the ones with the lowest and highest Young's modulus of 71.4 ±2.9 and 181.2±7.1 MPa, respectively. This result shows that the orientation of the fibres directly influences the mechanical properties of the P(VDF-TrFE) membranes, where oriented fibre membranes lead to higher Young's modules, when stretched in the direction of the fibres [40]. Similar high Young's modules are also presented by the porous TIPS P(VDF-TrFE) membranes before and after wetted. On the other hand, comparing the RO-ES P(VDF-TrFE) membranes with the *Whatman™ no.1* substrates, both featuring randomly oriented fibres, the former are characterized by a much higher Young's modulus, when wet, indicating that PVDF-based membranes show more suitable mechanical properties than cellulose for the present application. Moreover, although it was not possible to determine the Young's modulus of the *Millipore HF090* substrates, it should be noted that besides needing a support material, the nitrocellulose membrane itself breaks up very easily when, for example, a finger is passed over and must therefore be handled very carefully, contrarily to the NIPS P(VDF-TrFE) membranes with similar spherulitic-like porous structure that present high Young's modulus, similar to the RO-ES P(VDF-TrFE) membranes, in both dry and wet state. Combined with these excellent mechanical properties, it should be noted that P(VDF-TrFE) membranes can be repeatedly wetted and dried without losing their physicomechanical properties, allowing, therefore, cleaning and reuse.

Molecular weight, degree of crystallinity and microstructure strongly influence the mechanical properties of polymer-based membranes. The degree of crystallinity, calculated (see Section

2.4.1) from the thermograms of the P(VDF-TrFE) membranes presented in Figure 4c, remains approximately constant, 26±3%, regardless of the processing conditions and plasma treatment, being within the typical range of values obtained for this copolymer [41]. Moreover, no significant variation is observed in the melting transition (T_M) which occurs at 149.7±1.0 ºC. Thus, the variations of the mechanical properties are attributed just to the different morphological features of the P(VDF-TrFE) membranes.

Finally, the crystalline phases of the P(VDF-TrFE) membranes are identified in the infrared spectra presented in Figure 4d. All membranes show the characteristic vibration modes at 839, 886 and 1402 cm^{-1}, which identify the polymer crystallization in the trans TTT' highly polar chain confirmation. Because of its electroactive β-phase, these membranes can be further explored for active multifunctional microfluidic substrates, with added value compared to the passive commercial microfluidic ones [16,19].

3.2. Contact angle and capillary flow rate assays

The hydrophobic nature of P(VDF-TrFE) is a major drawback that must be overcome for its use as microfluidic substrates where capillary flow is essential. In this sense, various surface modification approaches can be applied to tailor the polymer surface wettability, such as plasma treatment, defluorination-sulfonation, surface coating/deposition, blending, and electron beam radiation, among others [4243]. Plasma treatment stands out as the most suitable method, due to their high versatility and for maintaining the main physicochemical properties of the polymer [30]. In this context, a reactive oxygen atmosphere allows to promote a stable hydrophilicity through the generation of carboxyl groups on the polymer surface by the incorporation of hydrophilic

functional groups [29] Thus, contact angle measurements over time were performed on the different substrates as a simple and effective method to quantify the wetting properties of the surfaces. A surface is commonly named hydrophobic when its water contact angle is higher than 90º, whereas values lower that 90º are associated with hydrophilic surfaces. Superhydrophobic and superhydrophilic are terms also used to characterize surfaces that features contact angles higher that 150º and lower than 10º, respectively [44]. The water contact angle values of the processed P(VDF-TrFE) w/o and w/ plasma treatment, along with the ones for the commercial substrates, are presented in Figure 5a.

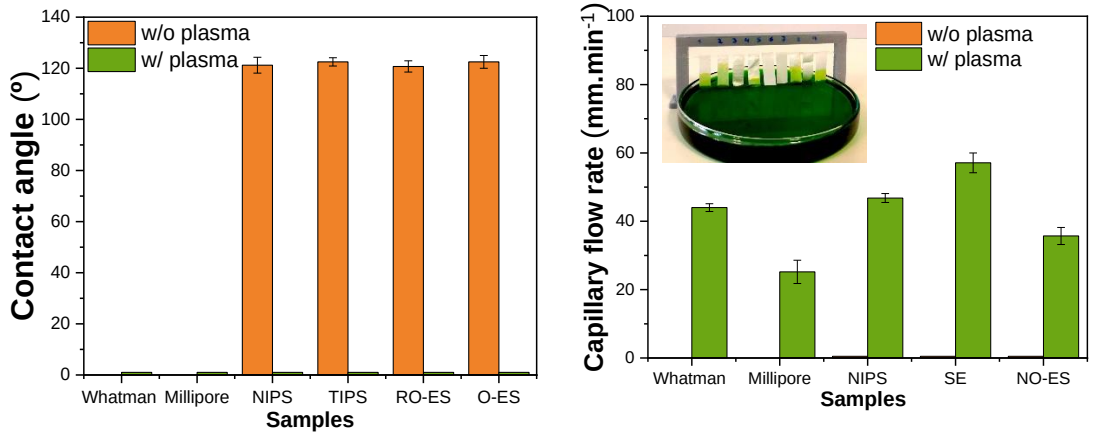

Figure 5. a) Contact angle and b) capillary flow rates in the "antigravity" direction of a dye solution for the commercial substrates and P(VDF-TrFE) membranes before and after oxygen plasma treatment; inset: Representative photograph of an experimental assay.

Commercial *Whatman™ no.1* and *Millipore H090* substrates are superhydrophilic. In turn, the processed P(VDF-TrFE) membranes present hydrophobic properties with contact angle of

~122±2º, independently of the morphology. After oxygen plasma treatment, the P(VDF-TrFE) membranes become superhydrophilic and are stable for at least 2 months.

Capillary flow rate assays were then performed as described in Section 2.4.2. This experiment validates the ability of the membranes to be used as microfluidic substrates, where passive capillary flow must occur preventing the need of any external actuation systems. The results are presented in Figure 5b. As anticipated, no flow was observed in the as-processed hydrophobic P(VDF-TrFE) membranes. In turn, plasma treated P(VDF-TrFE) membranes feature capillary flow rates varying from 35.7±2.5 $mm.min^{-1}$ to 88.3±3.7 $mm.min^{-1}$, corresponding to the plasma treated RO-ES and plasma treated O-ES P(VDF-TrFE) membranes, respectively. This result demonstrates that, besides the type of porous morphology, the orientation of the fibres has a direct effect on the capillary flow rate, the highest value being obtained for the O-ES membranes due to the orientation of the fibres along the length of the strip. Comparing the plasma treated NO-ES P(VDF-TrFE) membranes and the commercial *Whatman™ no.1* substrates, with similar randomly oriented fibre morphologies, the obtained capillary flow rates are slightly higher for the *Whatman™* samples with values of 44.1±1.1 $mm.min^{-1}$ compared to 35.7±2.5 $mm.min^{-1}$ for the NO-ES P(VDF-TrFE) membranes, which can be attributed to the more compact structure of the *Whatman™* membranes that allows higher flow rates. In turn, the spherulitic-like porous structure of the plasma treated NIPS P(VDF-TrFE) membranes present capillary flow rates of 46.8±1.3 $mm.min^{-1}$, higher than the ones obtained for *Millipore HF090* membranes with similar morphology (25±3.4 $mm.min^{-1}$). This behaviour can be attributed to the polymer melted and recrystallized regions caused by the plasma treatment that increase the contact areas for the fluid to flow and thus allow faster flow rates. Finally, plasma treated porous TIPS P(VDF-TrFE) membranes feature capillary flow rates of 57.1±2.9 $mm.min^{-1}$, an intermediate value between all

measured samples. Thus, the capillary flow rate of the P(VDF-TrFE) membranes can be adapted and tailored by varying their morphology and/or fibre orientation, which is relevant in order to match process requirements (such as collection, separation, pre-concentration, among others) in microfluidic substrates.

3.3. Proof-of-concept: colorimetric glucose determination

Colorimetric analysis allows to determine the presence or even concentration of a specific chemical entity in a solution based on a colour variation. This method is widely used in clinical analysis laboratories, for industrial purposes such as analysis of water contaminants and also in POC/portable analytical systems. In the scope of this research, colorimetric assays based on the quantification of glucose were performed on commercial *Whatman™ no.1* and *Millipore HF090* substrates, as well as on the plasma treated P(VDF-TrFE) membranes with different morphologies to evaluate their performance as microfluidic substrates. First, an optimized microfluidic design was printed using a wax printer for the quantification of glucose in the range of 25 to 100 $mg.dL^{-1}$, as described in Section 2.4.3. Scanned images of the microfluidic systems after the glucose assays are presented in Figure 6a and their corresponding calibration curves as well as the extrapolated linear fittings are shown in Figures 6b and 6c, respectively. For that, mean grey values are presented as a function of the logarithm of the glucose concentration.

Whatman™	*Millipore*	NIPS	TIPS	RO-ES	O-ES

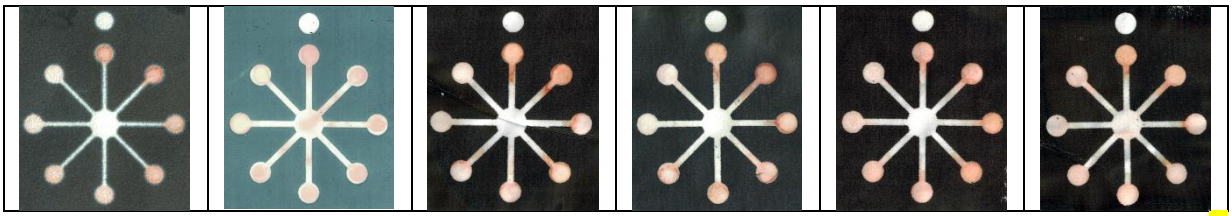

a)

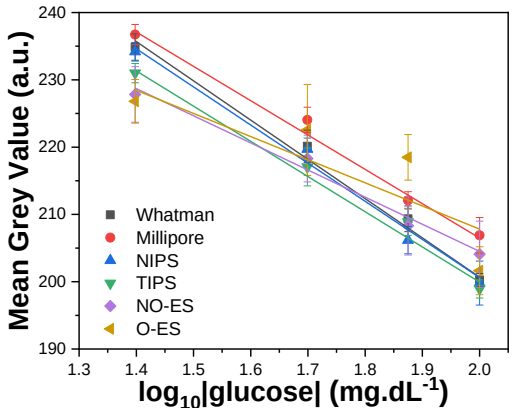

b)

$$y = m \times x + b$$

	m	b	R^2
Whatman™ no.1	-58.4	317.5	0.994
Millipore HF090	-51.0	308.5	0.985
NIPS w/ plasma	-56.7	313.9	0.994
TIPS w/ plasma	-52.3	304.5	0991
RO-ES w/ plasma	-40.3	285.1	0.989
O-ES w/ plasma	-34.4	276.6	0.746

c)

Figure 6. a) Representative scanned images of commercial substrates and plasma treated P(VDF-TrFE) membranes after glucose assays. *Millipore HF090* substrates were evaluated on the baking side and the image horizontally inverted. For identification of glucose concentration see Figure 2; b) Calibration curves of glucose for commercial substrates and plasma treated P(VDF-TrFE) membranes. The results are presented as mean grey values and corresponding standard deviation measured on the reaction chambers of the microfluidic substrates using *ImageJ* software according to the method described in ref. [37]; c) Corresponding linear fitting.

With respect to the wax print quality, it is confirmed that all microfluidic substrates present good resolution, with the exception of the *Whatman™ no.1* substrates where the wax expands ~1.2 mm during the thermal post-treatment. This behaviour may affect the capillary flow rate and thus attention must be paid when *Whatman™ no.1* substrates are used in combination with wax printing, according to the applications requirements[39,45–47].

Regarding the colours generated after the colorimetric assays, they only appear on the back side in the case of the *Millipore HF090* substrates, remaining completely white on the front side. Thus, scanned images of the *Millipore HF090* in Figure 6a represent the back side and the image was horizontally inverted in order to present colour intensities and thus glucose concentrations in the same reaction chambers as the other substrates. Figure 6a confirms that the plasma treated P(VDF-TrFE) substrates feature good wax printing resolution and colour formation on the front side. In all colorimetric assays, the grey intensity in the reaction chambers (corresponding to the red colour in Figure 6a, for proper identification) intensifies with increasing glucose concentration. However, the homogeneity of the colour generated in the reaction chambers varies depending on the substrate, which directly affects the quality of the obtained calibration curves (Figures 6b e 6c). Very good linear fittings were obtained with the *Whatman^{TM} no.1* substrates and plasma treated NIPS and TIPS P(VDF-TrFE) membranes with R^2 higher than 0.990, followed by the plasma treated RO-ES P(VDF-TrFE) and *Millipore HF090* with R^2 of 0.989 and 0.985, respectively.

Higher slope associated with higher sensitivity was obtained with the *Whatman^{TM} no.1* substrates and plasma treated NIPS P(VDF-TrFE) membranes with values of -58.4 and -56.7, respectively. This small variation demonstrates that the expansion of the wax during the thermal post-treatment in the *Whatman^{TM} no.1* substrates did not affect significantly the colorimetric reaction, in this specific application.

The worst fitting was obtained with the plasma treated O-ES P(VDF-TrFE) membranes that may result from the orientation of the fibres were the unidirectional flow leads to the heterogeneous formation of the coloured solution in the reaction chamber that feature a circular shape. This behaviour along with the capillary flow rate presented in Figure 6b indicate that P(VDF-TrFE)

membranes based on oriented fibres show high potential for unidirectional capillary flow of solutions/entities at higher rate but are not the most indicated for colorimetric quantification using more isotropic microfluidic design. Thus, with the exception of the orientation of the fibres and printing quality, the variation in the porous morphology of the microfluidic substrates does not appear to have a significant effect on the quality of colorimetric assays.

3.4. Comparative assessment and final remarks

According to the presented and discussed results, Table 1 summarizes the relevant properties of the developed P(VDF-TrFE) membranes and the commercial *Whatman™ nº.1* and *Millipore HF090* substrates for microfluidic applications.

Table 1. Comparative characteristics of commercial and P(VDF-TrFE) membranes as substrates for microfluidic applications.

	Whatman™ nº.1	***Millipore HF090***	**P(VDF-TrFE) membranes**			
Morphology	Randomly oriented cellulose microfibres	Spherulitic-like nitrocellulose porous structure (laminated membrane with backing material)	Spherulitic-like structure (by NIPS)	Porous structure (by TIPS)	Randomly oriented fibres structure (by ES)	Oriented fibres structure (by ES)
Wettability	Superhydrophilic	Superhydrophilic	Superhydrophilic after plasma treatment			
Capillary flow (mm.min^{-1})	44±1.13	25.2±3.4 *	46.8±1.3	57.1±2.9	35.7±2.5	88.3±3.7
Wax print quality	Poor (expands 1.2	High	High			

	mm after curing)					
Colorimetric detection quality	Good	Good (only in the back side)	Good	Good	Good	Bad (heterogeneous)
Mechanical properties (dry/wet)	+/-	+/+**	+/+	+/+	+/+	+/+
Reusable	No	No	Yes (washable)			
Smart/active Properties	No	No	Electroactive (piezo-, pyro and ferroelectric)			

*tailorable according to Millipore type
**need backing material and scrapes easily

Although commercial *Whatman™ no.1* and *Millipore HF090* substrates are commonly used for the manufacture of portable analytical systems, some limitations were presented within the scope of this study and potential innovative solutions based on superhydrophilic P(VDF-TrFE) membranes were highlighted. In fact, the properties that most differentiate the processed P(VDF-TrFE) membranes when compared to the commercial ones evaluated in this work are related to the tailorable morphology, with a direct effect on the capillary flow rate, the high wax print quality, the homogeneous generation of a colour reaction related to the concentration of the entities (except for the O-ES) and the excellent mechanical properties both in dry and wet conditions. Moreover, the plasma treated P(VDF-TrFE) membranes can be washed and dried repeatedly without losing their physicochemical properties, allowing their reuse, which can be interesting for specific applications and with respect to circular economy and sustainability considerations (as an example, preventing waste and one time use by washing and reuse of the substrates). Finally, P(VDF-TrFE) membranes feature electroactive properties (piezo-, pyro- and ferroelectric) [48], which can be further explored in a future generation of microfluidic substrates with smart and/or (multi)functional properties.

4. Conclusions

Poly(vinylidene-*co*-trifluorethylene) (P(VDF-TrFE)) membranes with tailored morphologies, including spherulitic, porous, randomly oriented and oriented fibres were produced for microfluidic applications. Some of the morphologies were selected to mimic the commercial *Whatman™ no. 1* cellulose filter paper with randomly oriented cellulose fibres and *Hi-Flow Plus* membranes *HF090* from *Millipore,* with a spherulitic-like nitrocellulose porous structure, both commonly used as microfluidic substrates. The P(VDF-TrFE) membranes were characterized and compared to the commercial ones in terms of physicochemical properties, capillary flow rate and microfluidic systems for the colorimetric glucose quantification were fabricated and evaluated. The main limitations of commercial substrates are their poor mechanical properties when wet (Young's modulus of 0.5±0.1 MPa), poor wax print quality (expansion of ~1.2 mm after curing) for the *Whatman™ no.1* substrates and the need for a backing substrate in the case of *Millipore HF090*. Although hydrophobic by nature, the P(VDF-TrFE) membranes become superhydrophilic after oxygen plasma treatment. The suitability of the plasma-treated P(VDF-TrFE) membranes as alternative or complementary to the commercially available substrates for microfluidic applications is demonstrated based on their tailorable morphology, tailorable capillary flow rate (from 35.7±2.5 $mm.min^{-1}$ to 88.3 $mm.min^{-1}$), high wax print quality and excellent mechanical properties (Young's modulus from 71.4±2.9 to 163.4±5.1 MPa in the wet state), allowing to match process requirements of specific (bio)technological applications (such as collection, separation, pre-concentration, mixing, among others). Beyond those properties, P(VDF-TrFE) membranes can be re-used after a cleaning process, and their electroactive properties makes them suitable for the development of a new generation of eco-friendly and

smart microfluidic substrates, as demonstrated in the present work by their use for the colorimetric quantification of glucose.

Corresponding Author

* senentxu.lanceros@bcmaterials.net;

* vanessa@dei.uminho.pt

Author Contributions

The manuscript was written through contributions of all authors. All authors have given approval to the final version of the manuscript.

Notes

The authors declare no conflict of interest.

ACKNOWLEDGMENT

This work was supported by the Portuguese Foundation for Science and Technology (FCT) under strategic funding UID/FIS/04650/2020, UIDB/04436/2020, UIDP/04436/2020 and projects PTDC/EMD-EMD/28159/2017 (POCI-01-0145-FEDER-028159). The authors also thank the FCT for financial support under grant SFRH/BD/140698/2018 (R.B.P.) The authors also acknowledge funding from the Basque Government Industry and Education Departments under the ELKARTEK and PIBA (PIBA-2018-06) programs, respectively. Technical and human support provided by SGIker (UPV/EHU, MICINN, GV/EJ, EGEF and ESF) is gratefully

acknowledged. Finally, the authors also thank E. S. Pimentel, Dr. J. Borges and Prof. F. Vaz for experimental support.

REFERENCES

(1) Nayak, S.; Blumenfeld, N. R.; Laksanasopin, T.; Sia, S. K. Point-of-Care Diagnostics: Recent Developments in a Connected Age. *Analytical Chemistry*. American Chemical Society January 2017, pp 102–123. https://doi.org/10.1021/acs.analchem.6b04630.

(2) Chaiyo, S.; Apiluk, A.; Siangproh, W.; Chailapakul, O. High Sensitivity and Specificity Simultaneous Determination of Lead, Cadmium and Copper Using MpAD with Dual Electrochemical and Colorimetric Detection. *Sensors Actuators, B Chem.* **2016**, *233*, 540–549. https://doi.org/10.1016/j.snb.2016.04.109.

(3) Busin, V.; Wells, B.; Kersaudy-Kerhoas, M.; Shu, W.; Burgess, S. T. G. Opportunities and Challenges for the Application of Microfluidic Technologies in Point-of-Care Veterinary Diagnostics. *Molecular and Cellular Probes*. Academic Press October 2016, pp 331–341. https://doi.org/10.1016/j.mcp.2016.07.004.

(4) Cinti, S.; Basso, M.; Moscone, D.; Arduini, F. A Paper-Based Nanomodified Electrochemical Biosensor for Ethanol Detection in Beers. *Anal. Chim. Acta* **2017**, *960*, 123–130. https://doi.org/10.1016/j.aca.2017.01.010.

(5) Zhu, H.; Fohlerová, Z.; Pekárek, J.; Basova, E.; Neužil, P. Recent Advances in Lab-on-a-Chip Technologies for Viral Diagnosis. *Biosensors and Bioelectronics*. Elsevier Ltd April 2020, p 112041. https://doi.org/10.1016/j.bios.2020.112041.

(6) Yetisen, A. K.; Akram, M. S.; Lowe, C. R. Paper-Based Microfluidic Point-of-Care Diagnostic Devices. *pubs.rsc.org* **2013**, *13*, 2210. https://doi.org/10.1039/c3lc50169h.

(7) Byrnes, S.; Thiessen, G.; Fu, E. Progress in the Development of Paper-Based Diagnostics for Low-Resource Point-of-Care Settings. *Bioanalysis*. November 2013, pp 2821–2836. https://doi.org/10.4155/bio.13.243.

(8) Martinez, A. W.; Phillips, S. T.; Butte, M. J.; Whitesides, G. M. Patterned Paper as a Platform for Inexpensive, Low-Volume, Portable Bioassays. *Angew. Chemie* **2007**, *119* (8), 1340–1342. https://doi.org/10.1002/ange.200603817.

(9) Carrell, C.; Kava, A.; Nguyen, M.; Menger, R.; Munshi, Z.; Call, Z.; Nussbaum, M.; Henry, C. Beyond the Lateral Flow Assay: A Review of Paper-Based Microfluidics. *Microelectron. Eng.* **2019**, *206*, 45–54. https://doi.org/10.1016/j.mee.2018.12.002.

(10) Yang, Y.; Noviana, E.; Nguyen, M. P.; Geiss, B. J.; Dandy, D. S.; Henry, C. S. Paper-Based Microfluidic Devices: Emerging Themes and Applications. *ACS Publ.* **2016**, *89* (1), 71–91. https://doi.org/10.1021/acs.analchem.6b04581.

(11) Zhang, A. L.; Zha, Y. Fabrication of Paper-Based Microfluidic Device Using Printed Circuit Technology. *AIP Adv.* **2012**, *2* (2). https://doi.org/10.1063/1.4733346.

(12) Xia, Y.; Si, J.; Li, Z. Fabrication Techniques for Microfluidic Paper-Based Analytical Devices and Their Applications for Biological Testing: A Review. *Biosensors and Bioelectronics*. Elsevier Ltd March 2016, pp 774–789. https://doi.org/10.1016/j.bios.2015.10.032.

(13) Pimentel, E. S.; Brito-Pereira, R.; Marques-Almeida, T.; Ribeiro, C.; Vaz, F.; Lanceros-Mendez, S.; Cardoso, V. F. Tailoring Electrospun Poly(l -Lactic Acid) Nanofibers as Substrates for Microfluidic Applications. *ACS Appl. Mater. Interfaces* **2020**, *12* (1), 60–69. https://doi.org/10.1021/acsami.9b12461.

(14) Ribeiro, C.; Costa, C. M.; Correia, D. M.; Nunes-Pereira, J.; Oliveira, J.; Martins, P.;

Gonçalves, R.; Cardoso, V. F.; Lanceros-Méndez, S. Electroactive Poly(Vinylidene Fluoride)-Based Structures for Advanced Applications. *Nat. Protoc.* **2018**, *13* (4), 681–704. https://doi.org/10.1038/nprot.2017.157.

(15) Gonçalves, R.; Cardoso, V. F.; Pereira, N.; Oliveira, J.; Nunes-Pereira, J.; Costa, C. M.; Lanceros-Méndez, S. Evaluation of the Physicochemical Properties and Active Response of Piezoelectric Poly(Vinylidene Fluoride- Co-Trifluoroethylene) as a Function of Its Microstructure. *J. Phys. Chem. C* **2018**, *122* (21), 11433–11441. https://doi.org/10.1021/acs.jpcc.8b02605.

(16) Zhao, B.; Cui, X.; Ren, W.; Xu, F.; Liu, M.; Ye, Z. G. A Controllable and Integrated Pump-Enabled Microfluidic Chip and Its Application in Droplets Generating. *Sci. Rep.* **2017**, *7* (1), 1–8. https://doi.org/10.1038/s41598-017-10785-1.

(17) Zhang, Y.; Wang, Y.; Jia, J.; Wang, J. Nonenzymatic Glucose Sensor Based on Graphene Oxide and Electrospun NiO Nanofibers. *Sensors Actuators, B Chem.* **2012**, *171–172*, 580–587. https://doi.org/10.1016/j.snb.2012.05.037.

(18) Pullano, S.; Mahbub, I.; Islam, S.; Fiorillo, A. PVDF Sensor Stimulated by Infrared Radiation for Temperature Monitoring in Microfluidic Devices. *Sensors* **2017**, *17* (4), 850. https://doi.org/10.3390/s17040850.

(19) Cardoso, V. F.; Knoll, T.; Velten, T.; Rebouta, L.; Mendes, P. M.; Lanceros-Méndez, S.; Minas, G. Polymer-Based Acoustic Streaming for Improving Mixing and Reaction Times in Microfluidic Applications. *RSC Adv.* **2014**, *4* (9). https://doi.org/10.1039/c3ra46420b.

(20) Cardoso, V. F.; Lopes, A. C.; Botelho, G.; Lanceros-Méndez, S. Poly(Vinylidene Fluoride-Trifluoroethylene) Porous Films: Tailoring Microstructure and Physical Properties by Solvent Casting Strategies. *Soft Mater.* **2015**, *13* (4), 243–253.

https://doi.org/10.1080/1539445X.2015.1083444.

(21) Sun, B.; Long, Y. Z.; Zhang, H. D.; Li, M. M.; Duvail, J. L.; Jiang, X. Y.; Yin, H. L. Advances in Three-Dimensional Nanofibrous Macrostructures via Electrospinning. *Progress in Polymer Science*. Elsevier Ltd May 2014, pp 862–890. https://doi.org/10.1016/j.progpolymsci.2013.06.002.

(22) Correia, D. M. M.; Ribeiro, C.; Sencadas, V.; Vikingsson, L.; Oliver Gasch, M.; Gómez Ribelles, J. L. L.; Botelho, G.; Lanceros-Méndez, S. Strategies for the Development of Three Dimensional Scaffolds from Piezoelectric Poly(Vinylidene Fluoride). *Mater. Des.* **2016**, *92*, 674–681. https://doi.org/10.1016/j.matdes.2015.12.043.

(23) Pawde, S. M.; Deshmukh, K. Surface Characterization of Air Plasma Treated Poly Vinylidene Fluoride and Poly Methyl Methacrylate Films. *Polym. Eng. Sci.* **2009**, *49* (4), 808–818. https://doi.org/10.1002/pen.21319.

(24) Cardoso, V. F.; Rocha, J. G.; Serrado Nunes, J.; Lanceros-Mendez, S.; Minas, G. Piezoelectric β-PVDF Polymer Films as Fluid Acoustic Microagitator. In *IEEE International Symposium on Industrial Electronics*; 2008; pp 2028–2033. https://doi.org/10.1109/ISIE.2008.4677095.

(25) Sencadas, V.; Ribeiro, C.; Nunes-Pereira, J.; Correia, V.; Lanceros-Méndez, S. Fiber Average Size and Distribution Dependence on the Electrospinning Parameters of Poly(Vinylidene Fluoride-Trifluoroethylene) Membranes for Biomedical Applications. *Appl. Phys. A Mater. Sci. Process.* **2012**, *109* (3), 685–691. https://doi.org/10.1007/s00339-012-7101-5.

(26) California, A.; Cardoso, V. F.; Costa, C. M.; Sencadas, V.; Botelho, G.; Gómez-Ribelles, J. L.; Lanceros-Mendez, S. Tailoring Porous Structure of Ferroelectric Poly(Vinylidene

Fluoride-Trifluoroethylene) by Controlling Solvent/Polymer Ratio and Solvent Evaporation Rate. *Eur. Polym. J.* **2011**, *47* (12), 2442–2450. https://doi.org/10.1016/j.eurpolymj.2011.10.005.

(27) Ferreira, J. C. C.; Monteiro, T. S.; Lopes, A. C.; Costa, C. M.; Silva, M. M.; Machado, A. V.; Lanceros-Mendez, S. Variation of the Physicochemical and Morphological Characteristics of Solvent Casted Poly(Vinylidene Fluoride) along Its Binary Phase Diagram with Dimethylformamide. *J. Non. Cryst. Solids* **2015**, *412*, 16–23. https://doi.org/10.1016/j.jnoncrysol.2015.01.003.

(28) Correia, D. M.; Ribeiro, C.; Botelho, G.; Borges, J.; Lopes, C.; Vaz, F.; Carabineiro, S. A. C.; MacHado, A. V.; Lanceros-Méndez, S. Superhydrophilic Poly(l-Lactic Acid) Electrospun Membranes for Biomedical Applications Obtained by Argon and Oxygen Plasma Treatment. *Appl. Surf. Sci.* **2016**, *371*, 74–82. https://doi.org/10.1016/j.apsusc.2016.02.121.

(29) Correia, D. M.; Ribeiro, C.; Sencadas, V.; Botelho, G.; Carabineiro, S. A. C.; Ribelles, J. L. G.; Lanceros-Méndez, S. Influence of Oxygen Plasma Treatment Parameters on Poly(Vinylidene Fluoride) Electrospun Fiber Mats Wettability. *Prog. Org. Coatings* **2015**, *85*, 151–158. https://doi.org/10.1016/j.porgcoat.2015.03.019.

(30) Correia, D. M.; Nunes-Pereira, J.; Alikin, D.; Kholkin, A. L.; Carabineiro, S. A. C.; Rebouta, L.; Rodrigues, M. S.; Vaz, F.; Costa, C. M.; Lanceros-Méndez, S. Surface Wettability Modification of Poly(Vinylidene Fluoride) and Copolymer Films and Membranes by Plasma Treatment. *Polymer (Guildf).* **2019**, *169*, 138–147. https://doi.org/10.1016/j.polymer.2019.02.042.

(31) Costa, C. M.; Rodrigues, L. C.; Sencadas, V.; Silva, M. M.; Rocha, J. G.; Lanceros-Méndez,

S. Effect of Degree of Porosity on the Properties of Poly(Vinylidene Fluoride-Trifluorethylene) for Li-Ion Battery Separators. *J. Memb. Sci.* **2012**, *407–408*, 193–201. https://doi.org/10.1016/j.memsci.2012.03.044.

(32) Tan, Q.; Li, S.; Ren, J.; Chen, C. Fabrication of Porous Scaffolds with a Controllable Microstructure and Mechanical Properties by Porogen Fusion Technique. *Int. J. Mol. Sci.* **2011**, *12* (2), 890–904. https://doi.org/10.3390/ijms12020890.

(33) Clements, J.; Davies, G. R.; Ward, I. M. A Broad-Line Nuclear Magnetic Resonance Study of a Vinylidene Fluoride/Trifluoroethylene Copolymer. *Polymer (Guildf).* **1992**, *33* (8), 1623–1629. https://doi.org/10.1016/0032-3861(92)91058-A.

(34) Lam, T.; Devadhasan, J. P.; Howse, R.; Kim, J. A Chemically Patterned Microfluidic Paper-Based Analytical Device (C-MPAD) for Point-of-Care Diagnostics. *Sci. Rep.* **2017**, *7* (1). https://doi.org/10.1038/s41598-017-01343-w.

(35) Abe, K.; Suzuki, K.; Citterio, D. Inkjet-Printed Microfluidic Multianalyte Chemical Sensing Paper. *Anal. Chem.* **2008**, *80* (18), 6928–6934. https://doi.org/10.1021/ac800604v.

(36) Lu, Y.; Shi, W.; Qin, J.; Lin, B. Fabrication and Characterization of Paper-Based Microfluidics Prepared in Nitrocellulose Membrane by Wax Printing. *Anal. Chem.* **2010**, *82* (1), 329–335. https://doi.org/10.1021/ac9020193.

(37) Shangguan, J.-W.; Liu, Y.; Wang, S.; Hou, Y.-X.; Xu, B.-Y.; Xu, J.-J.; Chen, H.-Y. Paper Capillary Enables Effective Sampling for Microfluidic Paper Analytical Devices. *ACS Sensors* **2018**, *3* (7), 1416–1423. https://doi.org/10.1021/acssensors.8b00335.

(38) Yamada, K.; Shibata, H.; Suzuki, K.; Citterio, D. Toward Practical Application of Paper-Based Microfluidics for Medical Diagnostics: State-of-the-Art and Challenges. *Lab Chip* **2017**, *17* (7), 1206–1249. https://doi.org/10.1039/c6lc01577h.

(39) Akyazi, T.; Basabe-Desmonts, L.; Benito-Lopez, F. Review on Microfluidic Paper-Based Analytical Devices towards Commercialisation. *Anal. Chim. Acta* **2018**, *1001*, 1–17. https://doi.org/10.1016/j.aca.2017.11.010.

(40) Maciel, M. M.; Ribeiro, S.; Ribeiro, C.; Francesko, A.; Maceiras, A.; Vilas, J. L.; Lanceros-Méndez, S. Relation between Fiber Orientation and Mechanical Properties of Nano-Engineered Poly(Vinylidene Fluoride) Electrospun Composite Fiber Mats. *Compos. Part B Eng.* **2018**, *139*, 146–154. https://doi.org/10.1016/j.compositesb.2017.11.065.

(41) Costa, C. M.; Rodrigues, L. C.; Sencadas, V.; Silva, M. M.; Lanceros-Méndez, S. Effect of the Microsctructure and Lithium-Ion Content in Poly[(Vinylidene Fluoride)-Co-Trifluoroethylene]/Lithium Perchlorate Trihydrate Composite Membranes for Battery Applications. *Solid State Ionics* **2012**, *217*, 19–26. https://doi.org/10.1016/j.ssi.2012.04.011.

(42) Liu, F.; Hashim, N. A.; Liu, Y.; Abed, M. R. M.; Li, K. Progress in the Production and Modification of PVDF Membranes. *J. Memb. Sci.* **2011**, *375* (1–2), 1–27. https://doi.org/10.1016/j.memsci.2011.03.014.

(43) Kang, G.-D.; Cao, Y.-M. Application and Modification of Poly(Vinylidene Fluoride) (PVDF) Membranes - A Review. *J. Memb. Sci.* **2014**, *463*, 145–165. https://doi.org/10.1016/j.memsci.2014.03.055.

(44) Otitoju, T. A.; Ahmad, A. L.; Ooi, B. S. Superhydrophilic (Superwetting) Surfaces: A Review on Fabrication and Application. *J. Ind. Eng. Chem.* **2017**, *47*, 19–40. https://doi.org/10.1016/j.jiec.2016.12.016.

(45) Carrilho, E.; Martinez, A. W.; Whitesides, G. M. Understanding Wax Printing: A Simple Micropatterning Process for Paper-Based Microfluidics. *Anal. Chem.* **2009**, *81* (16), 7091–

7095. https://doi.org/10.1021/ac901071p.

(46) Renault, C.; Koehne, J.; Ricco, A. J.; Crooks, R. M. Three-Dimensional Wax Patterning of Paper Fluidic Devices. *Langmuir* **2014**, *30* (23), 7030–7036. https://doi.org/10.1021/la501212b.

(47) Younas, M.; Maryam, A.; Khan, M.; Nawaz, A. A.; Jaffery, S. H. I.; Anwar, M. N.; Ali, L. Parametric Analysis of Wax Printing Technique for Fabricating Microfluidic Paper-Based Analytic Devices (MPAD) for Milk Adulteration Analysis. *Microfluid. Nanofluidics* **2019**, *23* (3). https://doi.org/10.1007/s10404-019-2208-z.

(48) Cardoso, V. F.; Costa, C. M.; Minas, G.; Lanceros-Mendez, S. Improving the Optical and Electroactive Response of Poly(Vinylidene Fluoride-Trifluoroethylene) Spin-Coated Films for Sensor and Actuator Applications. *Smart Mater. Struct.* **2012**, *21* (8). https://doi.org/10.1088/0964-1726/21/8/085020.

TABLE OF CONTENT